Supporting Information

Acid-induced Nitrite Reduction of a Nonheme Iron(II)-Nitrite: Mimicking biological Fe-NiR Reaction

Kulbir,[a] Sandip Das,[a] Tarali Devi,[c] Somnath Ghosh,[a] Subash Chandra Sahoo,[b] Pankaj Kumar*[a]

[a]Department of Chemistry, Indian Institute of Science Education and Research (IISER), Tirupati 517507, India

[b]Department of Chemistry, Punjab University, Punjab, Chandigarh, India

[c]Humboldt-Universität zu Berlin, Institut für Chemie, Brook-Taylor-Straße 2, D-12489 Berlin, Germany

* To whom correspondence should be addressed.

E-mail: pankaj@iisertirupati.ac.in

Table of Contents

Materials: All the reagents and solvents obtained from commercial sources (Sigma Aldrich Chemical Co. and Tokyo Chemical Industry) were of the best available purity and used without further purification unless otherwise indicated. Solvents were dried according to reported literature and distilled under an inert atmosphere before use.[S1] $Na^{15}NO_2$ (99.2% ^{15}N-enriched) was purchased from ICON Services Inc. (Summit, NJ, USA). The 12TMC ligand was prepared by reacting excess amounts of formaldehyde and formic acid with 1,4,7,10-tetraazacyclododecane as reported previously.[S2]

Instrumentation: UV-vis spectra were recorded on an Agilent tech 8454 diode array spectrometer equipped with a thermostat cell holder (UNISOKU Scientific Instruments) designed for low-temperature experiments. FT-IR spectra in solid form were recorded on Bruker-Alpha Eco-ATR FTIR spectrometer using the standard KBr disk method. ^{1}H-NMR spectra were measured with a Bruker model Ascend 400 FT-NMR spectrometer. Electrospray ionization mass spectra (ESI-MS) were recorded on an Agilent Mass Spectrometer (6200 series TOF/6500 series Q-TOF B.08.00) by infusing samples directly into the source using a manual method. The spray voltage was set at 4.2 kV and the capillary temperature at 80 °C. GC-MS analyses were recorded on an Agilent 7890B GC system equipped with a 5977B MSD Mass analyser. Single crystal X-ray diffraction data were collected using Bruker D8 Venture super Duo diffractometer with Photon-III detector using Mo source (λ = 0.71073 Å) and on Super-Nova (Mo) X-ray diffractometer. EPR spectral data were collected using an X-band JEOL Model JES FA200 instrument at liquid nitrogen temperature.

Synthesis of [(12TMC)Fe^{II}(CH_3CN)](OTf)$_2$ (1). CH_3CN solution (2 mL) of Fe^{II}-triflate (480 mg, 1.1 mmol) was added to 12TMC (229 mg, 1 mmol) with constant stirring for 12 hours at room temperature under an Ar atmosphere (we usually prefer to synthesize in the Glove box) as reported elsewhere.[S3] The solution's color changed to pale yellow after reaction completion. The reaction mixture was dried under a vacuum, and the dried product was dissolved in DCM. Diethyl ether (50 mL) was added to precipitate **1** (white solid). The precipitate was collected and dried under a vacuum over anhydrous $CaCl_2$. Yield: 525 mg (~ 85 %). UV: λ_{max} = 333 nm (ε = 60 M^{-1} cm^{-1}).

Synthesis of [(12TMC)Fe^{II}(NO_2)](OTf) (2): To a 5 ml CH_3CN solution of [(12TMC)Fe^{II}(CH_3CN)](OTf)$_2$ (623 mg, 1 mmol), 1 mL solution of $NaNO_2$ (69 mg, 1 mmol) with 15-crown-5 (2.5 equivalent) in CH_3CN was added slowly with constant stirring under Ar atmosphere. The mixture was stirred for one hour at RT (298 K) until the color of the solution changed from colorless to deep yellow, indicating the completion of the reaction. The solvent

was removed under vacuum, and the residue was dissolved in DCM and then layered with diethyl ether and kept for crystallization at - 20 °C. Yield: 430 mg (~ 90%). UV: λ_{max} = 325 nm (ε = 356 M^{-1} cm^{-1}). FT-IR (KBr pellet): 2940, 1270, 1015, 757 cm^{-1}. Mass (*m/z*): Calcd: 330.1, Found: 330.1. [(12TMC)Fe^{II}($^{15}NO_2^-$)](OTf) (**2**-$^{15}NO_2^-$) was prepared by using the same method with $Na^{15}NO_2$. FT-IR (KBr pellet): 2940, 1247, 1015, 757 cm^{-1}. Mass (m/z): Calcd: 331.1, Found: 331.1.

Synthesis of Iron-nitrosyl species ({FeNO}^{7}, 3) (Reaction of 2 + H^+). Complex **3** was generated in the reaction of H^+-ion as per the following details, explained next. The synthesis of **3** can be done either using the Glove box /or using the schlenk line under Ar conditions. Upon addition of one-equiv. /or two-equiv. H^+ to the Ar saturated CH_3CN solution (10 mL) of [(12TMC)Fe^{II}(CH_3CN)]$(OTf)_2$ (0.480 g, 1 mmol), it showed a visual color change from deep-yellow to green. We then kept the reaction mixture for 15 minutes, and the solution was layered with Ar-saturated ether, and the solution was kept at 233 K to obtain complex **3** as crystals/solid. After two days, we obtained deep green colored crystals of [(12TMC)Fe^{II}(NO)]$(OTf)_2$, which was confirmed with different spectral parameters. We performed the same reactions several times to determine crude yields, and the average yield of **3** was confirmed to be 80 (± 4) %. We also determined the single-crystal structure of complex **3**, which showed an axially coordinated end-on NO moiety with a Co-N-O bond angle of 168.65 Å, suggesting a radical behavior of NO moiety. UV: λ_{max} = 350 nm (ε = 1450 $M^{-1}cm^{-1}$) at 233 K in CH_3CN. FT-IR (KBr pellet): 2940, 1783 cm^{-1}. Mass (*m/z*): Calcd: 464.1, Found: 464.1 ([(12TMC)Fe^{II}(NO)(OTf)]$^+$).

Synthesis of {FeNO}^{7} (Reaction of 1 + NO gas). To compare the spectroscopic data of {FeNO}^{7} (**3**) generated in the reaction of **2** + H^+ (triflic acid), we have prepared an authentic {FeNO}^{7} by reacting **1** with $NO_{(g)}$ directly. The details are explained next. We have reacted [(12TMC)Fe^{II}(CH_3CN)]$(OTf)_2$ (0.623 g, 1 mmol) in Ar-saturated CH_3CN (10 mL) with an excess of $NO_{(g)}$ for 5 min, and the color of the solution was changed from colorless to green color. The reaction mixture was kept for 30 min, and excess $NO_{(g)}$ was removed by purging Ar gas (degassing) at 233 K, and then we layered it with Ar-saturated ether. Deep green colored crystals [(12TMC)Fe(NO)]$(OTf)_2$ were obtained by slow diffusion after several days at 233 K. UV: λ_{max} = 350 nm (ε = 1450$M^{-1}cm^{-1}$) at 233 K in CH_3CN. FT-IR (KBr pellet): 2940, 1783 cm^{-1}. Mass (*m/z*): Calcd: 464.1, Found: 464.1 ([(12TMC)Fe^{II}(NO)(OTf)]$^+$).

Reactivity Studies: We follow multiple spectral measurements to avoid discrepancies in the spectroscopic data. Hence, all UV-vis spectral measurements were run in a UV cuvette in

CH_3CN at specific temperatures. All kinetic reactions were run at least three times, and the data reported here are the average outcome for these reactions. We have performed all the reactions using CH_3CN as solvent at room temp (298 K) as well as 233 K. The formation of **3** with H_2O_2 /or H_2O in the reactions was identified by comparing with authentic samples, and product yields were calculated by comparing with standard curves prepared with original samples. In addition, NMR measurements were performed under the Ar atmosphere at specific temperatures to follow the formation of H_2O /H_2O_2 and also the confirmation of magnetic moments of metal centers using Evans' method.

$^{14/15}$N-labeling Experiments by FT-IR Spectroscopy (Reduction of NO_2^- to NO): To follow the change in the functional groups (NO_2^- to NO) coordinated to Fe-center and labeling N-atom, we have recorded the FT-IR spectra of the different complexes in their solid form as KBr pellets. The FT-IR spectra of **2** showed a nitrite ($^{14}NO_2^-$) characteristic peak at 1270 cm^{-1}, which shifted to 1247 cm^{-1} when prepared with ^{15}N-labeled nitrite ($^{15}NO_2^-$). The change in the IR stretching frequency of Fe-bound NO_2^- (Δ = 23 cm^{-1}) confirmed that an increase in the reduced mass of nitrogen atom (^{14}N to ^{15}N) is responsible for the decrease in the stretching frequency of the NO_2^- functional group. We observed similar spectral changes when the IR spectra of **3** were recorded with ^{14}N and ^{15}N-labeled atoms. The FT-IR spectra of **3** showed a characteristic nitrosyl stretching frequency at 1783 cm^{-1} (^{14}N), which shifted to 1755 cm^{-1} (^{15}N, Δ = 28 cm^{-1}) when exchanged with the ^{15}N-labeled nitrosyl functional group.

$^{14/15}$N-labeling Experiments by ESI-Mass Spectrometry (Reduction of NO_2^- to NO): In addition to the FT-IR spectral measurements, we have performed the ESI-MS spectral measurements to establish the N-atom source for **3** and **2**. The ESI-MS spectra for **2**-$^{14}NO_2^-$ and **2**-$^{15}NO_2^-$ showed scientific agreement with the labeled N-atom by showing an increase in the mass value for Fe^{II}-NO_2^- complexes ($[(12TMC)Fe(NO_2^-)]^+$ (calc. *m/z* 330.1) and $[(12TMC)Fe(^{15}NO_2^-)]^+$ (calc. *m/z* 331.1), respectively). We observed similar mass changes for **3** formed in the reaction of **2** with H^+. The ESI-MS spectrum of **3** showed a prominent peak at *m/z* 463.1, $[(12TMC)Fe(NO)(OTf)]^+$ (calc. *m/z* 463.1), and shifted to 464.1, $[(12TMC)Fe(^{15}NO)(OTf)]^+$ (calc. *m/z* 464.1), confirming the change of functional groups.

Magnetic moment calculation and determination of the spin-state of Fe-center in complexes 2 & 3: Evans' method of ^{1}H-NMR was performed to determine the spin state (number of unpaired electrons) of Fe-center in **2** and **3** at 298 K. A WILMAD® coaxial insert (with a sealed capillary) tubes containing only CD_3CN solvent (with 1.0% TMS) were inserted into the standard NMR tubes containing the **2** and **3** (4.0 mM, with 0.1% TMS), respectively.

We have calculated the chemical shift values of the TMS peak in the presence of **2** and/or **3** with respect to that of the TMS peak in the outer NMR tube. The magnetic moments for both complexes were calculated using the given equation. [S4]

2	**3**
$\mu_{eff} = 0.0618(\Delta\nu T / 2fM)^{1/2}$	$\mu_{eff} = 0.0618(\Delta\nu T / 2fM)^{1/2}$
$\mu_{eff} = 0.0618 * (76 * 298 / 2 * 400 * 0.004)^{1/2}$	$\mu_{eff} = 0.0618 * (16 * 298 / 2 * 400 * 0.004)^{1/2}$
$\boldsymbol{\mu_{eff}}$ **= 5.19 BM**	$\boldsymbol{\mu_{eff}}$ **= 2.3 BM**

Where f = oscillator frequency (MHz) of the superconducting spectrometer, T = absolute temperature, M = molar concentration of the **2** and **3**, and ν = difference in frequency (Hz) between the two TMS signals.

The calculated magnetic moments for **2** and **3** were determined to be 5.19 BM and 2.3 BM in CD_3CN at RT, respectively. These magnetic moment values suggest the presence of 4 unpaired electrons in the Fe^{2+} center of **2** (S = 2). While the presence of one unpaired electron in **3** (S = 1/2).

Calculation of Binding Constant (K_b): The binding constant values $K_b(Fe^{II}\text{-}NO_2^-)$ & $K_b(\{FeNO\}^7$ were determined by titrating the **1** to the different concentrations of NO_2^- & NO, respectively. The stock solutions of **1** (0.5 mM) were prepared in CH_3CN, and the reacting species/guest molecules were prepared in the required solvents in 5.0 mM ($NaNO_2$/crown ether in CH_3CN) & 14 mM ($NO_{(g)}$ in CH_3CN), respectively. Solutions of **1** with increasing concentration of the reacting species were prepared separately. These solutions' UV-vis spectra were recorded to get absorbance values as specific λ_{max} values. The binding constants were then calculated using the Benesi-Hildebrand equation. Binding constant values were determined from the equation given below.[S5]

$$1/(A\text{-}A_o) = 1/\{K_b(A_{max}–A_o)\,[X]_n\} + 1/[A_{max}\text{-}A_o]$$

Here, A_o is the absorbance of **1** in the absence of guests, A is the absorbance in the presence of guests at different concentrations, and A_{max} is the absorbance in the presence of added $[X]_{max}$ where X was NO_2^- /or NO, respectively, and K_b is the binding constant (M^{-1}). The binding constants (K_b) were determined from the slope of the straight line of the plot of 1/(A-Ao) against $1/(Amax–Ao)[X]_n$. The binding constants (K_b) as determined by the UV-vis titration method for **2**, $K_b(Fe^{II}\text{-}NO_2^-)$, & **3**, K_b ($\{FeNO\}^7$) with X are found to be 4.7×10^2 M^{-1} & 8.4×10^2 M^{-1} for NO_2^- and NO, respectively.

Qualitative and quantitative analysis of H_2O_2 by ^{1}H-NMR. To confirm and calculate the amount of the H_2O_2 formed upon reacting **2** with one-equiv. CF_3SO_3H, we have monitored the reaction by ^{1}H-NMR spectroscopy. In this regard, the ^{1}H-NMR spectrum of **2** (2.4 mg / 500 μL, 10 mM) with one-equiv. CF_3SO_3H in CD_3CN showed a signal at 8.66 ppm, corresponding to H_2O_2. We compared the ^{1}H-NMR spectrum of the H_2O_2 formed in the above reaction with the authentic samples, H_2O_2 only and H_2O_2 plus **3**, which established the formation of H_2O_2. Additionally, we have calculated the amount of H_2O_2 formed in the above reaction by comparing the peak-integral, corresponding to H_2O_2 (8.66 ppm) of the reaction mixture (**2** + CF_3SO_3H) with the authentic sample (5 mM H_2O_2 + **3**) containing an internal standard Benzene (5 mM). We have calculated the yield of H_2O_2, following the internal-standard method, in three different experiments to have an average value found to be 54.4 % (defining ½ equivalent of H_2O_2 relative to **2** as 100% yield). These calculations suggest that the lower yield of evolved H_2O_2 is due to its decomposition with time to other species.

S. No.	Reaction System	Integral of benzene peak (7.37 ppm) **(A)**	Integral of H_2O_2 peak (8.6 ppm) **(B)**	Ratio **(B)/(A)**
(a)	**3** + H_2O_2 (5 mM)	6	2	0.33
(b)	**2** + 1.1 equiv. H^+	6	1.1	0.183
(c)	**2** + 1.1 equiv. H^+	6	1.15	0.191
(d)	**2** + 1.1 equiv. H^+	6	1.0	0.166

Amount of H_2O_2 formed:

Sample 1 = (0.183 / 0.33) × 5 mM = 2.77 mM (55.4 %)

Sample 2 = (0.191 / 0.33) × 5 mM = 2.89 mM (57.8 %)

Sample 3 = (0.166 / 0.33) × 5 mM = 2.51 mM (50.2 %)

H_2O_2 formed in the reaction (average): = ~ 54.4 %

Estimation of H_2O_2 (*Iodometric-titration*): Additionally, the amount of H_2O_2 formed in the reaction of **2** with one-equiv. of H^+ was also calculated using iodometric titration. First, H_2O_2 was generated in the reaction of **2** (0.1 mM) with one-equiv. of H^+ (0.1 mM) in 2.5 mL CH_3CN under an Ar atmosphere at room temperature. The reaction solution was treated with an excess of sodium iodide (0.15 mM) under an Ar atmosphere, and the UV-vis spectrum was recorded for the reaction. As explained below, the quantity of I_3^- formed in the reaction was determined by finding an absorbance value at 361 nm as a result of I_3^- (λ_{max} = 361 nm, ε = 2.8 × 10^4 M^{-1} cm^{-1}).

Amount of H_2O_2 formed:

Sample 1 = (Abs. = 0.99) = 0.0353 mM (~ 70 % of H_2O_2)

Sample 2 = (Abs. = 0.95) = 0.0339 mM (~ 67.8 % of H_2O_2)

Sample 3 = (Abs. = 0.9) = 0.0321 mM (~ 64 % of H_2O_2)

H_2O_2 formed in the reaction (average): = ~ 67 % (defining ½ equivalent of H_2O_2 relative to **2** as 100% yield).

Also, we have determined the generation of H_2O_2 in the reaction of **2** (0.1mM) with two-equiv. H^+ (0.2 mM) under similar conditions. The reaction solution was treated with an excess of sodium iodide (0.15 mM) in 2.5 ml CH_3CN under an Ar atmosphere. The UV-vis spectrum was recorded for the reaction. H_2O_2 formed in the reaction was found in negligible amounts.

Detection of $[Fe\text{-}ONOH]^{2+}$ intermediate (•OH radical trapping experiment): We performed the •OH radical trapping experiment using 2,4-di-*tert*-butyl-phenol (2,4-DTBP) to confirm the formation of •OH radical from the N-O bond homolysis. For this reaction, we have reacted **2** (1.0 mM) with 2,4-DTBP (2.5 mM) in the presence of one-equiv. H^+ in CH_3CN at 293 K under Ar atmosphere. Then the qualitative and quantitative analysis of the reaction mixture was performed using GC-MS and HPLC, respectively. To quantify the different products forming in the reaction mixture, we used the standard plots of all the compounds in HPLC. In this experiment, we observed the formation of 3,5-Di-*tert*-butylcatechol (3,5-DTBC) with small amounts of 2,4-DTBP-dimer (3,5-DTBP-D) and nitro-2,4-DTBP (nitro-3,5-DTBP), suggesting the N-O bond homolysis to form free •OH radical and hence indirectly proving the presence of $[Fe\text{-}ONOH]^{2+}$ intermediate (**3**). The amount of 3,5-DTBC formed in the reaction

was found to be ~ 22 % (0.22 mM), accounting for 44 % •OH radical, 2,4-DTBP-D (~ 8 %, 0.04 mM, 16 % •OH radical), and nitro-2,4-DTBP (~ 6 %, 0.0198 mM, 18 % •OH radical) in the reaction mixture, because some amount of •OH decomposes to other side products due to its high reactivity. To confirm the source of •OH, we have performed a similar reaction using CF_3SO_3D instead of CF_3SO_3H. Here, we have observed the formation of 3,5-DTBC-D, confirming the source of •OH is **[**Fe-ONOH$]^{2+}$ intermediate. In addition, we generate [Fe-$^{16}O^{14}N^{18}OH]^{2+}$ intermediate species in the reaction of **2**-$^{16}O^{14}N^{18}O^-$ + H^+ and trap it using the 2,4-DTBP test. In the reaction mixture, we observed the formation of 3,5-DTBC(^{18}OH), with the formation of $^{16}O^{14}N^{18}O$-DTBP.

Monitoring reaction of 2 with H^+ using EPR spectroscopy: We followed the reaction of **2** with H^+ at different time intervals with EPR spectroscopic measurements. In this regard, an EPR tube equipped with 500 µl CH_3CN solution of **2** (4 mM) was prepared inside the glovebox and sealed with a rubber septum. The EPR tube was further cooled to 233 K, and an Ar-saturated solution of H^+ (two-equiv.) was added to the EPR tube using a gas-tight hamilton syringe, and the EPR spectrum was recorded at 77 K. After that, the tube was warmed to 233 K and re-recorded the spectrum at 77 K. This process continued until the reaction was completed to follow the reaction progress. Separately, we recorded an authentic sample of **3**. The EPR spectrum of isolated **3** (4 mM) in CH_3CN was recorded at 77 K under Ar.

Bond valance sum calculation. For more clearly in the oxidation state of **3**. We calculated the oxidation state of the Fe-center using the bond valance sum method using crystal parameters. z_j is the oxidation state of the metal center, S_{ij} is the bond valance for the bond between the *i* and *j* atom, Ro is constant R is the bond length between i and j atom, and B is constant for all bonds 0.37.[S6]

$$z_j = \sum S_{ij}$$

$$(S_{ij}) \text{ bond valence} = \exp((Ro-R)/B)$$

For BVS calculations, 3 was treated as Fe^{2+} as well as Fe^{3+}. Calculations suggest that when Fe is treated as Fe^{2+}, calculation showed it to have 1.846, while when it was treated as Fe^{3+}, it showed a 2.63 oxidation state. BVS calculations also support iron oxidation state as Fe^{2+}.

Nitric Oxide Preparation and Purification. Nitric oxide (NO) was prepared and purified by following a detailed procedure, as shown in Figure S21. First, NO gas was prepared by the reaction of $NaNO_2$ with H_2SO_4 under an Ar atmosphere and then passed through two different types of columns. First, it passes through a column filled with NaOH beads to remove higher nitrogen oxide impurities. After that, the NO passes through a set of two columns filled with

NaOH beads molecular sieves to remove the minor amount of remaining higher nitrogen oxides and moisture impurities. The highly purified $NO_{(g)}$ was then collected in a vacuum Schlenk flask fitted with a rubber septum (free from oxygen; after several cycles of vacuum and Ar purging). High pressure $NO_{(g)}$ (with pressure >1 atmosphere; the septum bulges outward due to high pressures) then passes through an Ar-saturated (oxygen-free) and dry Acetonitrile (CH_3CN) solution for 15 minutes. The concentration of NO in the NO-saturated CH_3CN solution is ~14 mM.[S7]

Single-Crystal XRD Studies. Single crystals suitable for diffraction studies were mounted on Hampton cryo-loops. All geometric and intensity data for the crystals were collected using a Super-Nova (Mo) X-ray diffractometer equipped with a micro-focus sealed X-ray tube Mo-Kα (λ =0.71073 A) X-ray source and HyPix3000 detector with increasing ω (width of 0.3 per frame) at a scan speed of either 5or 10 s/frame. The CrysAlisPro software was used for data acquisition and data extraction. Using Olex2[S8], the structure was solved with the SIR2004[S9] structure solution program using Direct Methods and refined with the ShelXL[S10] refinement package using Least Squares minimization. All non-hydrogen atoms were refined with anisotropic thermal parameters. There are two molecules per asymmetric unit, and one of the N-tetramethylated cyclam (TMC) ligand's ring is found to be highly disordered. Detailed crystallographic data and structural refinement parameters are summarized in Table T1 and T2. CCDC2181978 and CCDC2181979 contain supplementary crystallographic data. These data can be obtained free of charge from The Cambridge Crystallographic Data Centre.

References

S1. W. L. Armarego, *purification of laboratory chemicals*, Butterworth-Heinemann, **2017**.

S2. J. A. Halfen, V. G. Young, Jr., *Chem. Commun.,* **2003**, 2894-2895.

S3. Cho, J.; Jeon, S.; Wilson, S. A.; Liu, L. V.; Kang, E. A.; Braymer, J. J.; Lim, M. H.; Hedman, B.; Hodgson, K. O.; Valentine, J. S.; Solomon, E. I.; Nam, W., Structure and reactivity of a mononuclear non-haem iron(III)-peroxo complex. *Nature* **2011,** *478*, 502-5.

S4. Evans, D. F., 400. The determination of the paramagnetic susceptibility of substances in solution by nuclear magnetic resonance. *J. Chem. Soc.* **1959**, 2003-2005.

S5. Goswami, S.; Sen, D.; Das, N. K.; Fun, H. K.; Quah, C. K., A new rhodamine based colorimetric 'off-on' fluorescence sensor selective for Pd2+ along with the first bound X-ray crystal structure. *Chem Commun (Camb)* **2011,** *47*, 9101-3

S6. W. Liu and H. H. Thorp, *Inorg. Chem.*, **1993**, 32, 4102-4105.

S7. Young, C. L. Solubility Data Series Val. 8 Oxides of Nitrogen, International Union of Pure and Applied Chemistry (IUPAC), **1981**.

S8. Dolomanov, O. V.; Bourhis, L. J.; Gildea, R. J.; Howard, J. A. K.; Puschmann, H., OLEX2: a complete structure solution, refinement and analysis program. *J Appl Crystallogr* **2009,** *42*, 339-341

S9. Burla, M. C.; Caliandro, R.; Camalli, M.; Carrozzini, B.; Cascarano, G. L.; De Caro, L.; Giacovazzo, C.; Polidori, G.; Siliqi, D.; Spagna, R., IL MILIONE: a suite of computer programs for crystal structure solution of proteins. *J Appl Crystallogr* **2007,** *40*, 609-613

S10. Sheldrick, G. M., Crystal structure refinement with SHELXL. *Acta Crystallogr C Struct Chem* **2015,** *71*, 3-8

Table T1 Crystallographic data for **2** and **3**.

	2	**3**
Chemical formula	$C_{13}H_{28}F_3FeN_5O_5S$	$C_{16}H_{31}F_6FeN_6O_7S_2$
Formula weight	479.31	653.44
Wavelength /Å	0.71073	0.71073
Crystal system	monoclinic	monoclinic
Space group	$P2_1/c$	$P2_1/c$
T, K	293(2)	293(2)
a, Å	16.1966(5)	11.791(2)
b, Å	16.5801(5)	14.711(3)
c, Å	16.2444(5)	15.692(3)
α, °	90	90
β, °	100.654(3)	104.111(5)
γ, °	90	90
V/ $Å^3$	4287.1(2)	2639.7(9)
Z	8	4
Calculated density, g/cm^3	1.485	1.644
Abs. Coeff. $/mm^{-1}$	0.859	0.820
Reflections collected	37140	46121
Unique reflections	8656	4519
Refinement method	Least-squares on F^2	Least-squares on F^2
Data/restraints/parameters	8656/0/549	4519/0/348
Goodness-of-fit on F^2	1.110	1.196
Final *R* indices [$I > 2\sigma(I)$]	$R_1 = 0.0689$	$R_1 = 0.0756$,
	$wR_2 = 0.2301$	$wR_2 = 0.1800$
R indices (all data)	$R_1 = 0.1046$	$R_1 = 0.1150$,
	$wR_2 = 0.2304$	$wR_2 = 0.2012$

Table T2 Selected bond lengths (Å) and bond angles (°) for **2** and **3.**

2		**3**	
Fe1 O1	2.175(4)	Fe1 N1	1.999(7)
Fe1 O2	2.182(4)	Fe1 N2	2.031(6)
Fe1 N1	2.203(4)	Fe1 N3	2.023(6)
Fe1 N2	2.200(4)	Fe1 N4	2.031(6)
Fe1 N3	2.222(3)	Fe1 N5	1.692(6)
Fe1 N4	2.209(4)		
O1 Fe1 O2	51.7(2)	N1 Fe1 N2	86.3(3)
O1 Fe1 N1	129.2(2)	N1 Fe1 N3	148.9(3)
O1 Fe1 N2	94.2(2)	N1 Fe1 N4	85.7(2)
O1 Fe1 N3	95.3(2)	N2 Fe1 N4	146.7(2)
O1 Fe1 N4	132.3(2)	N3 Fe1 N2	84.8(3)
O2 Fe1 N3	129.1(2)	N3 Fe1 N4	85.5(3)
N1 Fe1 O2	95.9(2)	N5 Fe1 N1	102.7(3)
N1 Fe1 N3	131.18(15)	N5 Fe1 N2	105.8(3)
N2 Fe1 O2	131.3(2)	N5 Fe1 N3	108.4(3)
N2 Fe1 N1	79.69(16)	N5 Fe1 N4	107.5(3)
N2 Fe1 N3	80.67(15)	O1 N5 Fe1	168.6(6)
N4 Fe1 O2	95.7(2)		
N4 Fe1 N1	81.27(18)		
N4 Fe1 N2	130.54(16)		
N5 O1 Fe1	99.5(4)		

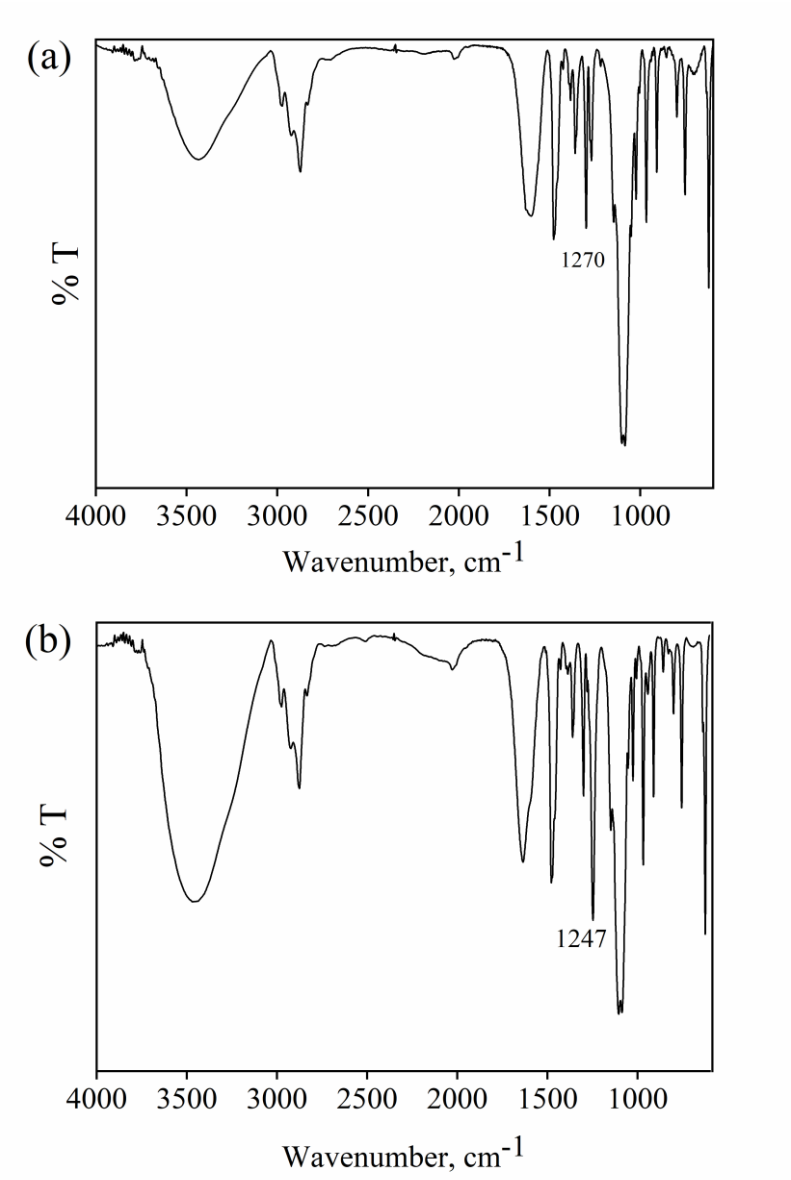

Figure S1. FT-IR spectrum of (a) **2** (with Fe^{II} bound $^{14}NO_2^-$) was recorded in the KBr pellet at 298 K. The spectrum showed the peaks for the aliphatic chain (at 2940 cm^{-1}) and Fe^{II}-bound $^{14}NO_2^-$ group (at 1270 cm^{-1}). (b) **2** (with Fe^{II} bound $^{15}NO_2^-$) recorded in KBr pellet at 298 K. The spectrum showed a peak Fe^{II}-bound $^{15}NO_2^-$ group (at 1247 cm^{-1}).

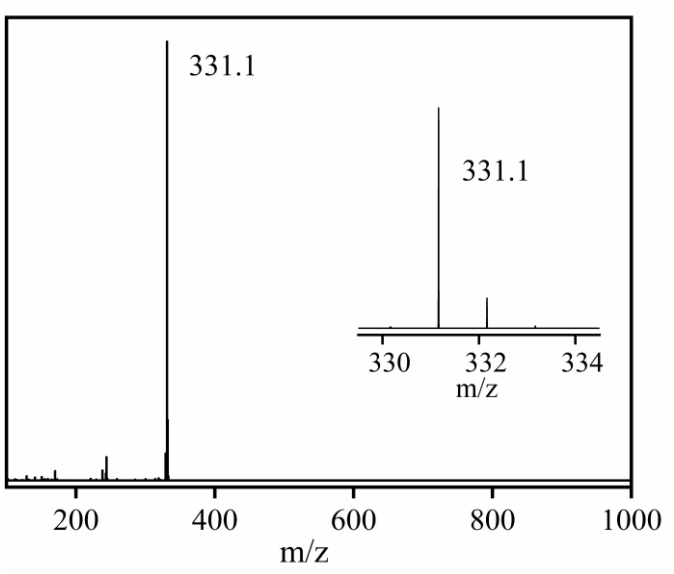

Figure S2. ESI-MS spectrum of **2** (with Fe^{II} bound $^{15}NO_2^-$). The peak at *m/z* 331.1 is assigned to be $[(12TMC)Fe^{II}(^{15}NO_2)]^+$, confirming a Fe^{II} bound $^{15}NO_2^-$ anion.

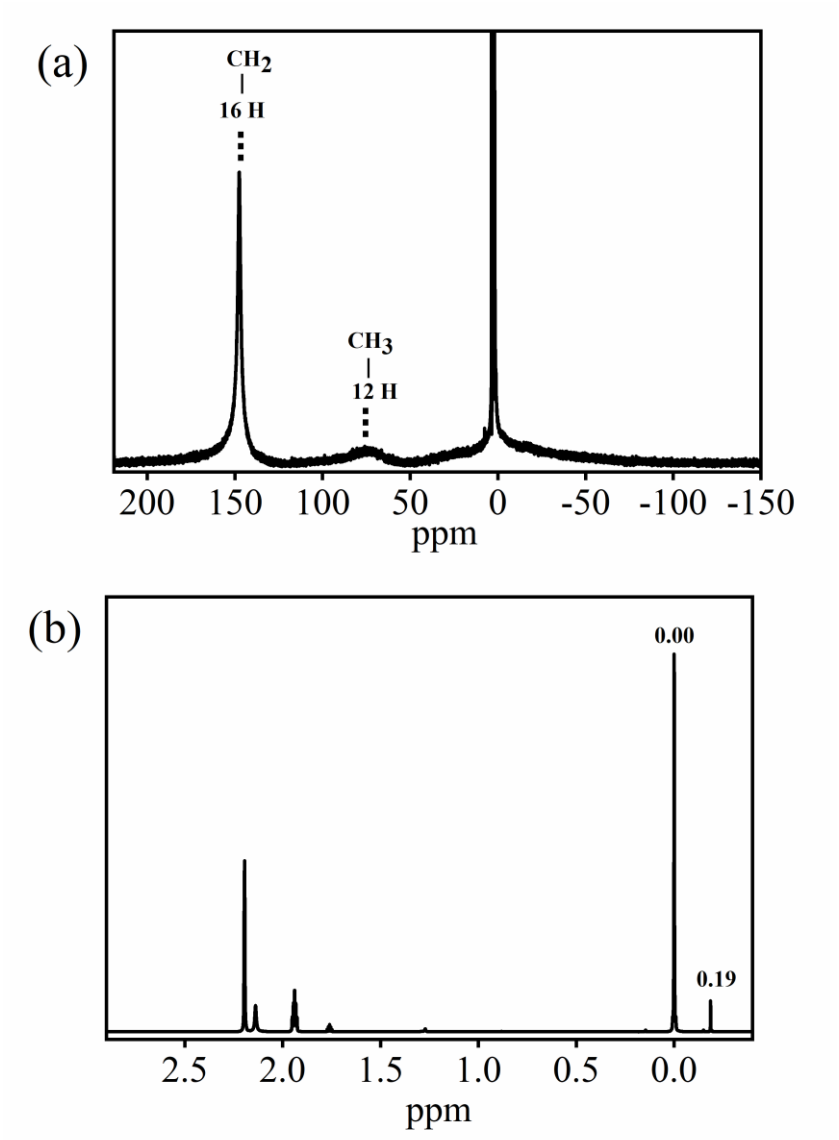

Figure S3. (a) Long-range ^{1}H-NMR (400 MHz) spectra of **2** (10 mM) in CD_3CN. (b) ^{1}H-NMR (400 MHz) spectrum of **2** (4 mM) in CD_3CN (0.1 % TMS), recorded in a coaxial NMR tube, with CD_3CN (1.0 % TMS) inside at RT.

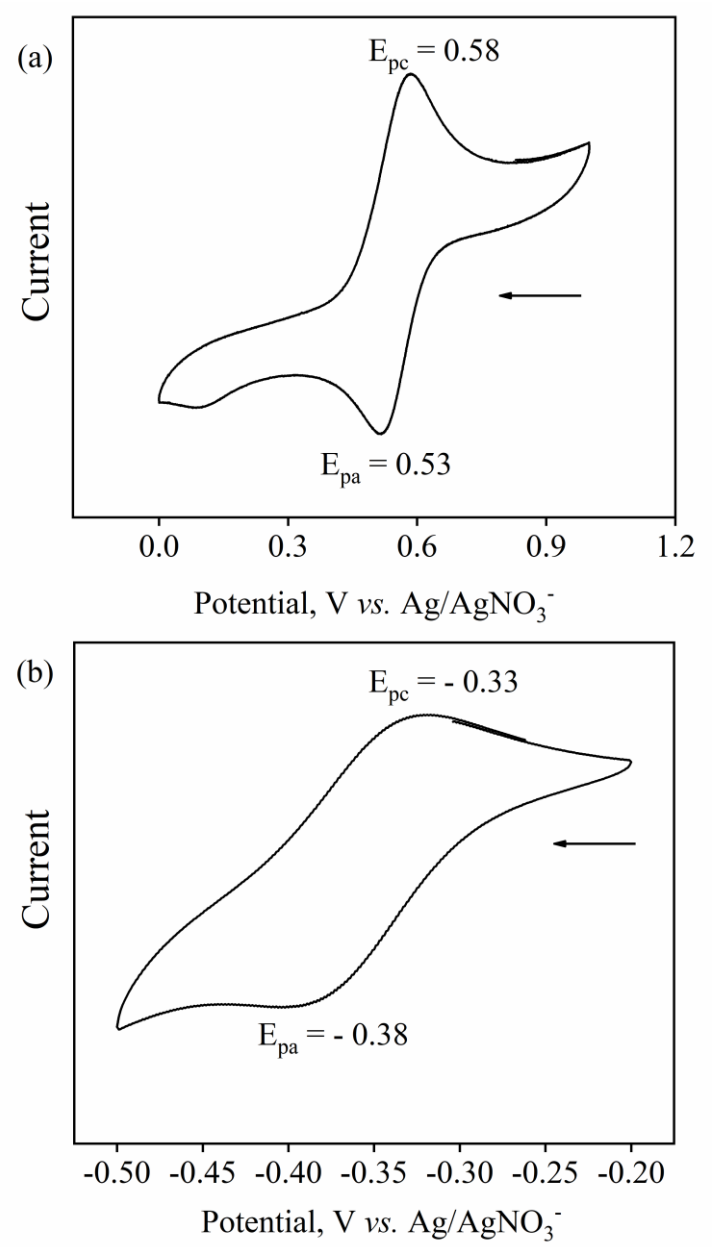

Figure S4. Cyclic voltammogram of (a) **2** (1 mM) and (b) **3** (1 mM) in CH_3CN containing n-Bu_4NPF_6 (0.25 M) as a supporting electrolyte (scan rate = 0.1 V/s) at 298 K.

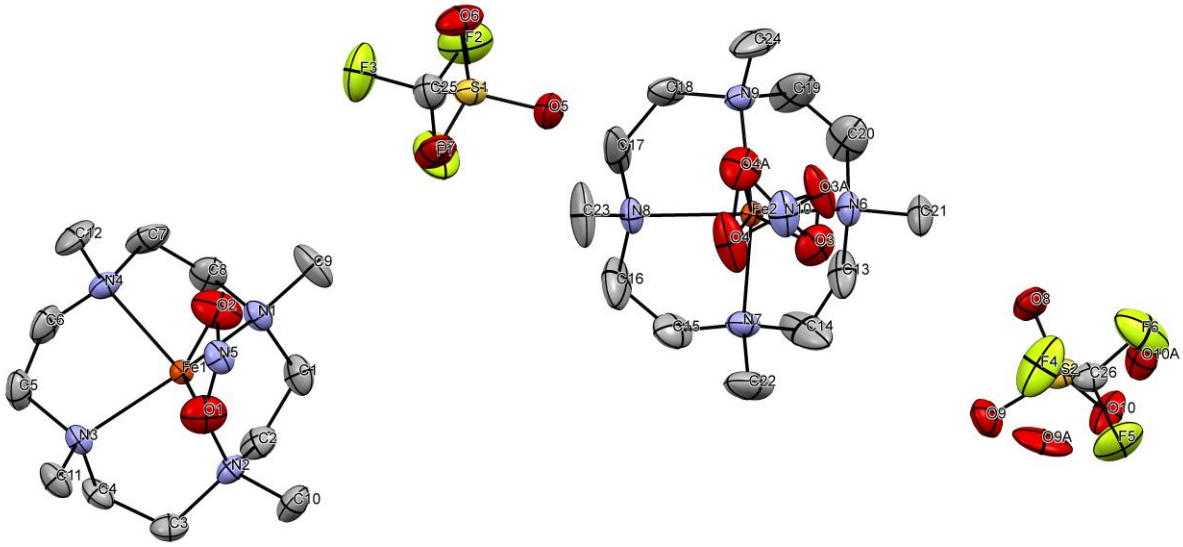

Figure S5. Displacement ellipsoid plots of **2** with 15 % probability. Hydrogen atoms are removed for better clarity.

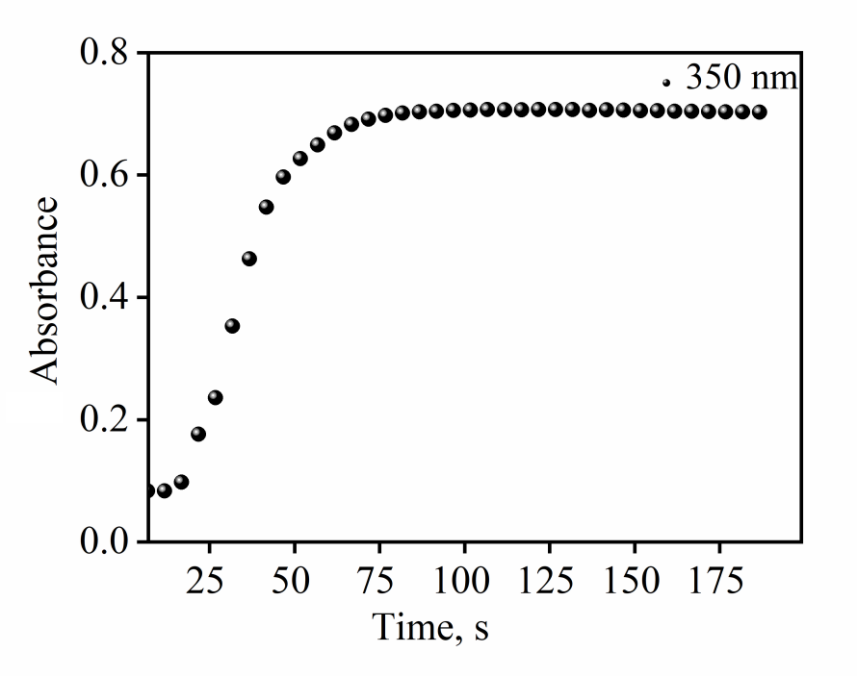

Figure S6. A time course of the formation of **3** (black circles). The reaction was monitored at 350 nm upon adding H^+ (one equiv.) to a solution of **2** (0.5 mM) in CH_3CN at 233 K.

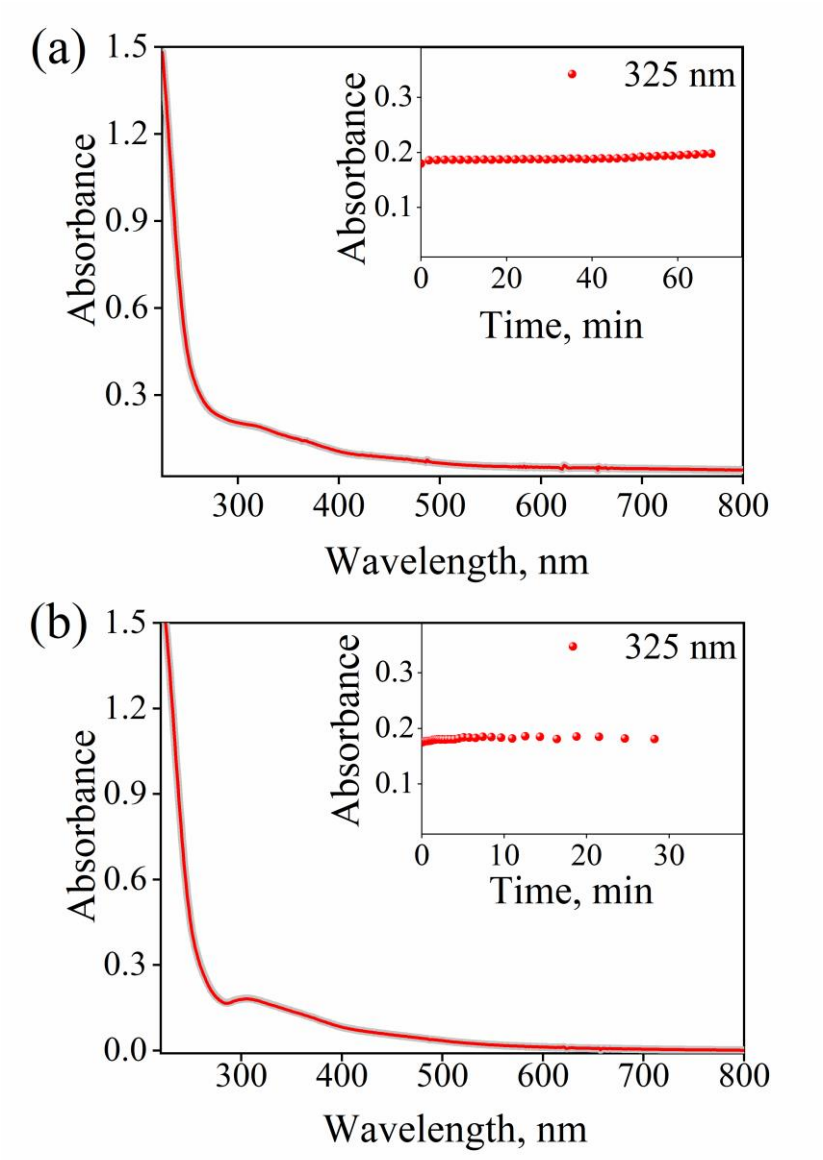

Figure S7. (a) UV-vis spectral changes of **2** (0.50 mM, Grayline to red line) in CH_3CN under Ar at 298 K. The inset shows the time course of the natural decay of **2** (red circles) monitored at 325 nm (b) UV-vis spectral changes of **2** (0.50 mM, Grayline to red line) upon the addition of tetrabutylammonium hydroxide (0.50 mM) in CH_3CN under Ar at 298 K. The inset shows the time course of the decay of **2** (red circles) monitored at 325 nm.

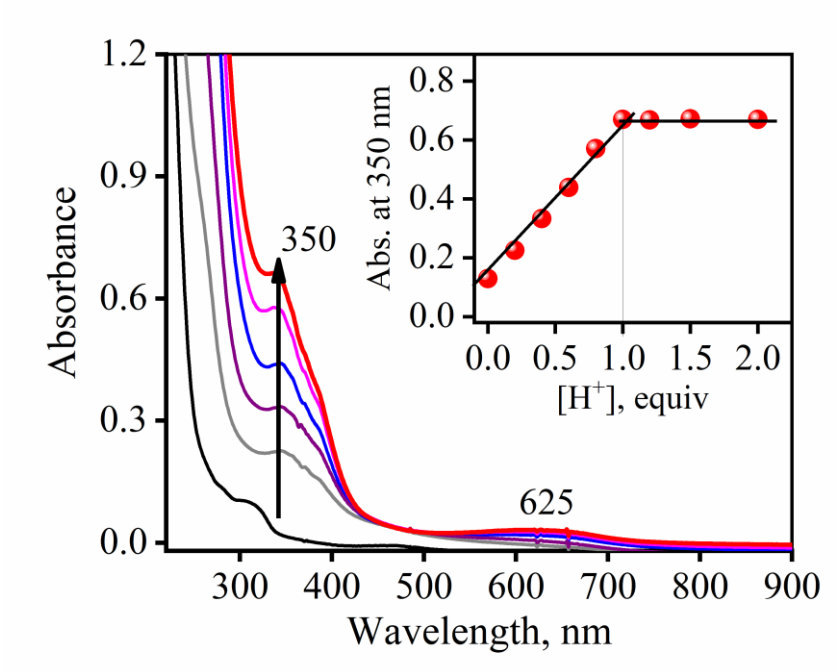

Figure S8. UV-vis spectral changes observed in the reaction **2** with H^+ (in the increments of 0, 0.20, 0.40, 0.60, 0.8, 1.0, 1.2, 1.5, 2 equiv.) in CH_3CN under Ar at 298 K.

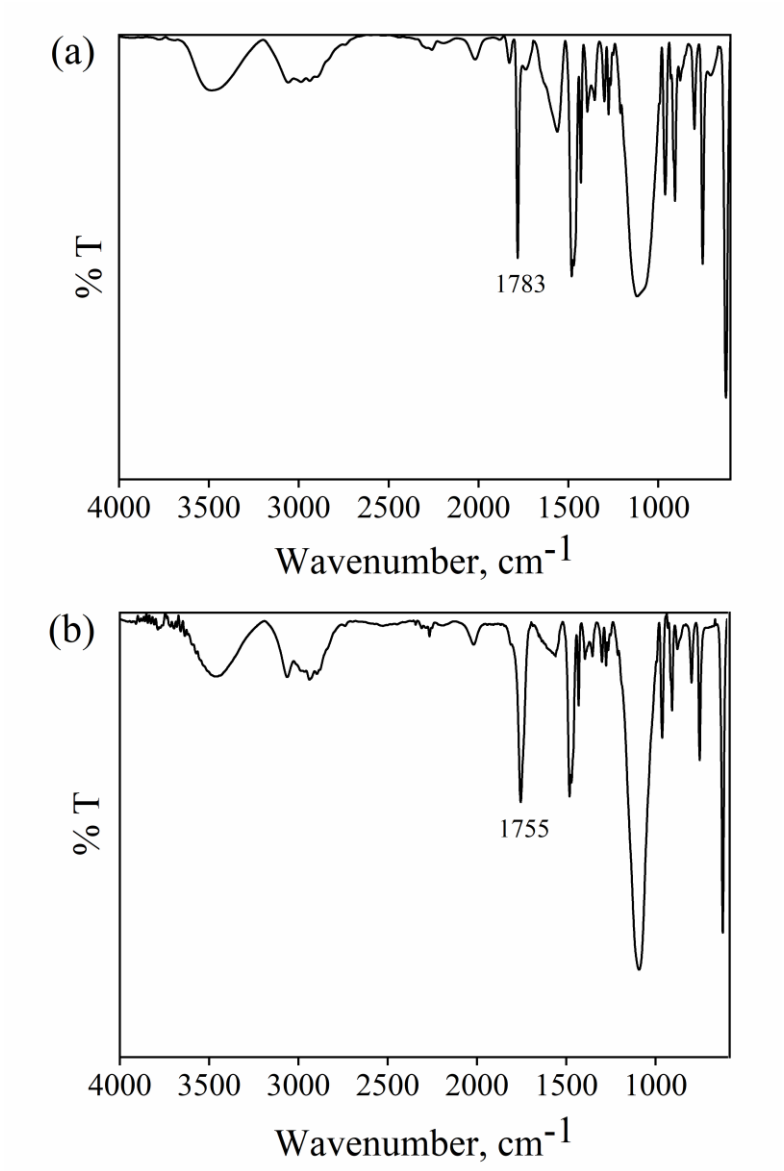

Figure S9. FT-IR spectrum of (a) **3** isolated from the reaction of **2** + H^+ recorded in KBr pellet at 298 K. The spectrum showed the peaks for the aliphatic chain (at 2940 cm^{-1}) and Fe-bound ^{14}NO moiety (at 1783 cm^{-1}). (b) **3** isolated from the reaction of **2** (with Fe^{II}-bound $^{15}NO_2^-$ anion) + H^+ recorded in KBr pellet at 298 K. The spectrum showed the peaks for Fe-bound ^{15}NO moiety (at 1755 cm^{-1}).

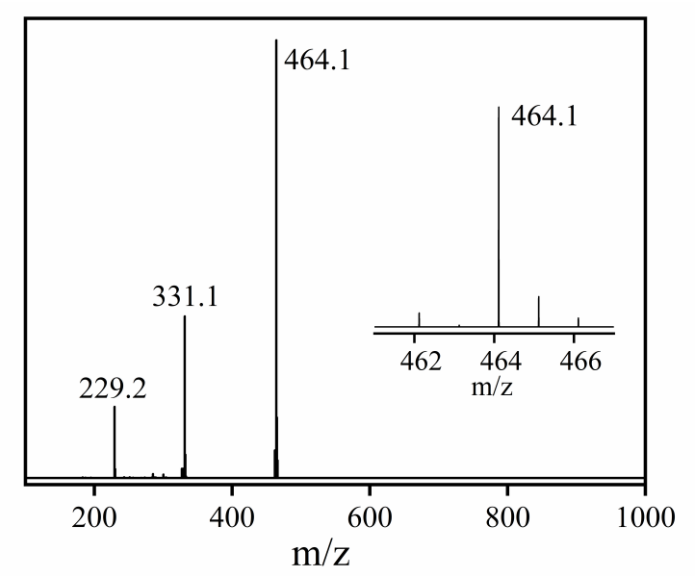

Figure S10. ESI-MS spectrum of **3**, formed in the reaction of **2** (with Fe^{II}-bound $^{15}NO_2^-$ anion) + H^+ (one- equiv.), in CH_3CN at 233K. The peak at *m/z* 464.1, 331.1, and 229.2 are assigned to be $[(12TMC)Fe(^{15}NO)(OTf)]^+$, $[(12TMC)Fe(^{15}NO_2^-)]^+$ and $[12TMC\text{-}H^+]^+$ (M+1), respectively.

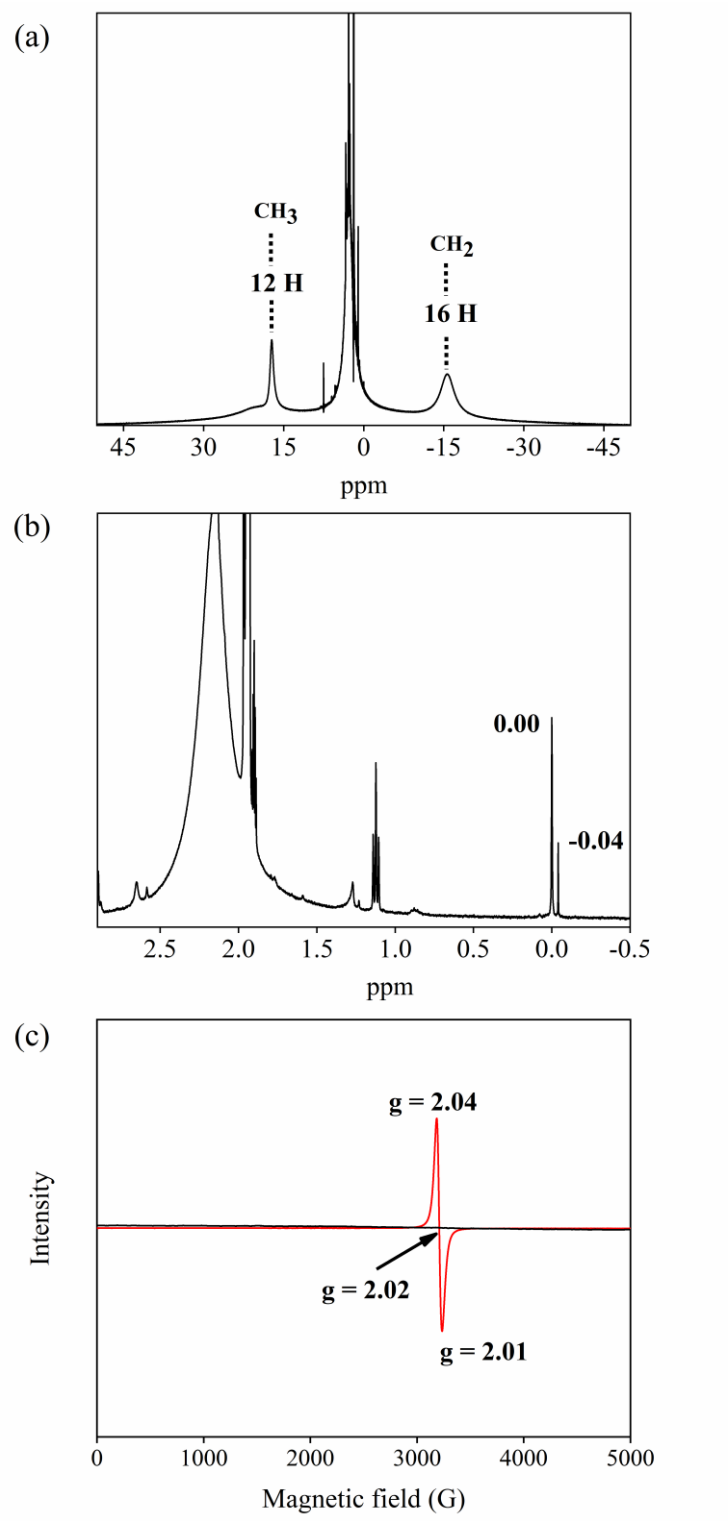

Figure S11. (a) Long-range ^{1}H-NMR (400 MHz) spectrum of the isolated product (**3**) from the reaction of **2** (20 mM) with H^{+} (one- equiv.) in CD_3CN. (b) ^{1}H-NMR (400 MHz) spectrum of **3** (4 mM) in CD_3CN (0.1 % TMS), recorded in a coaxial NMR tube, with inside CD_3CN (1.0 % TMS) at RT. (c) EPR of Isolated **3** (red line) and **2** (black line) in CH_3CN at 77 K.

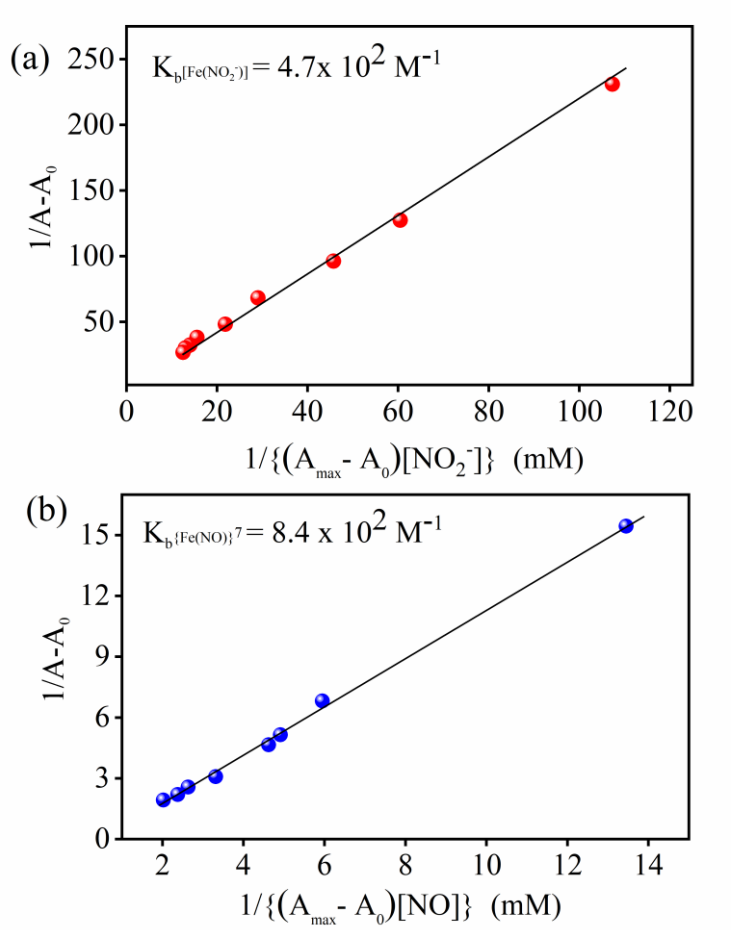

Figure S12. Binding constants values of (a) Fe^{II}-center bound NO_2^- in **2** and (b) Fe^{II}-center bound NO in **3**. These values were calculated using the Benesi-Hildebrand equation.

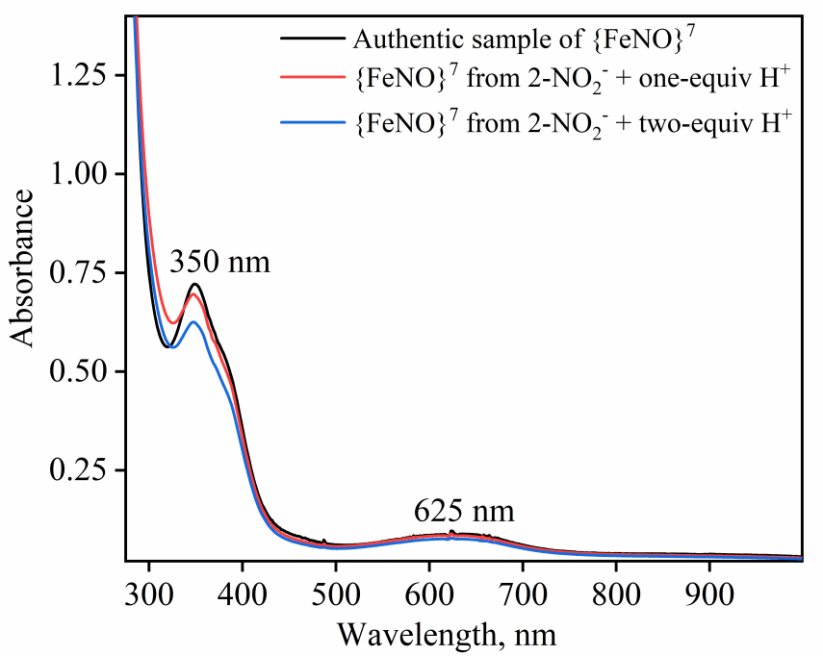

Figure S13. UV-vis spectral comparison of authentic sample **3** (black line) prepared from passing $NO_{(g)}$ to the CH_3CN solution of **1**, the reaction mixture of **2** + one equiv. H^+ (red line) in CH_3CN at 233 K and the reaction mixture of **2** + two equiv. H^+ (red line) in CH_3CN at 233 K.

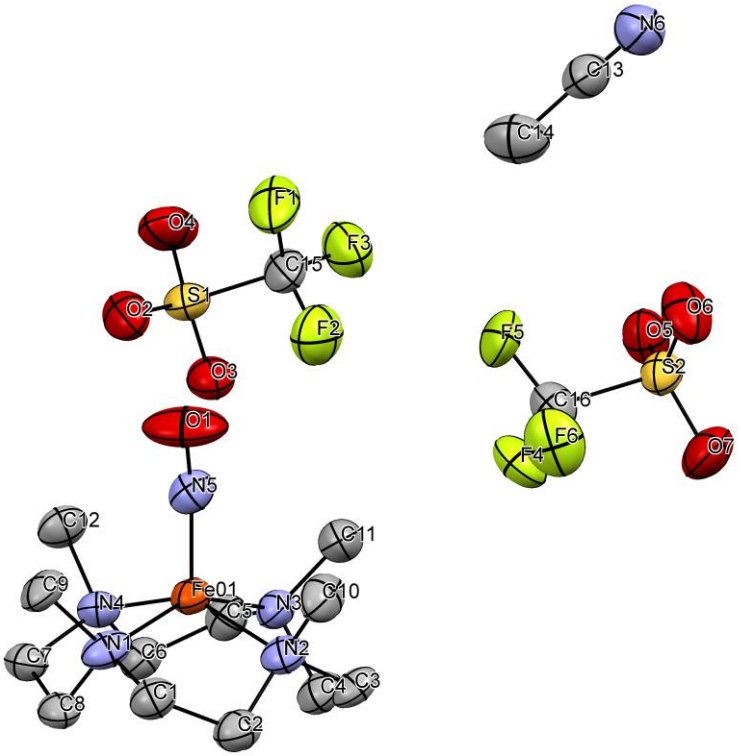

Figure S14. Displacement ellipsoid plots of **3** with 50 % probability. Disordered C-atoms in the TMC ring and the H atoms have been removed for clarity.

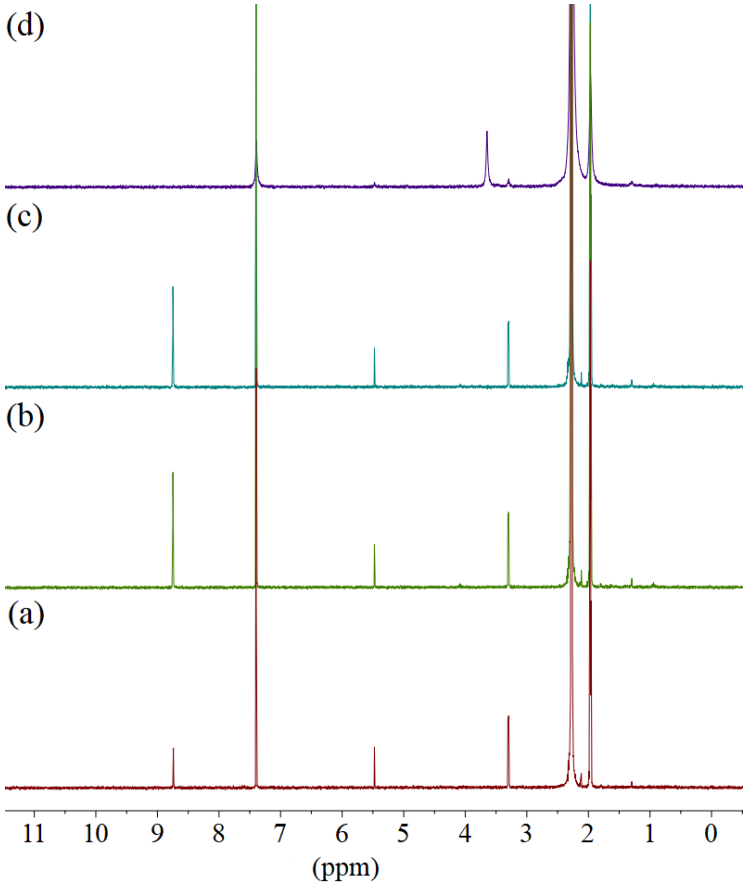

Figure S15. ^{1}H-NMR (400 MHz) spectra of (a) **2** (10 mM) + H^{+} (10 mM) (b) **3** (10 mM) + H_2O_2 (5 mM), (c) H_2O_2 (5mM), and (d) **2** (10 mM) + H^{+} (20 mM), having benzene (10 mM) as an internal standard in CD_3CN at RT.

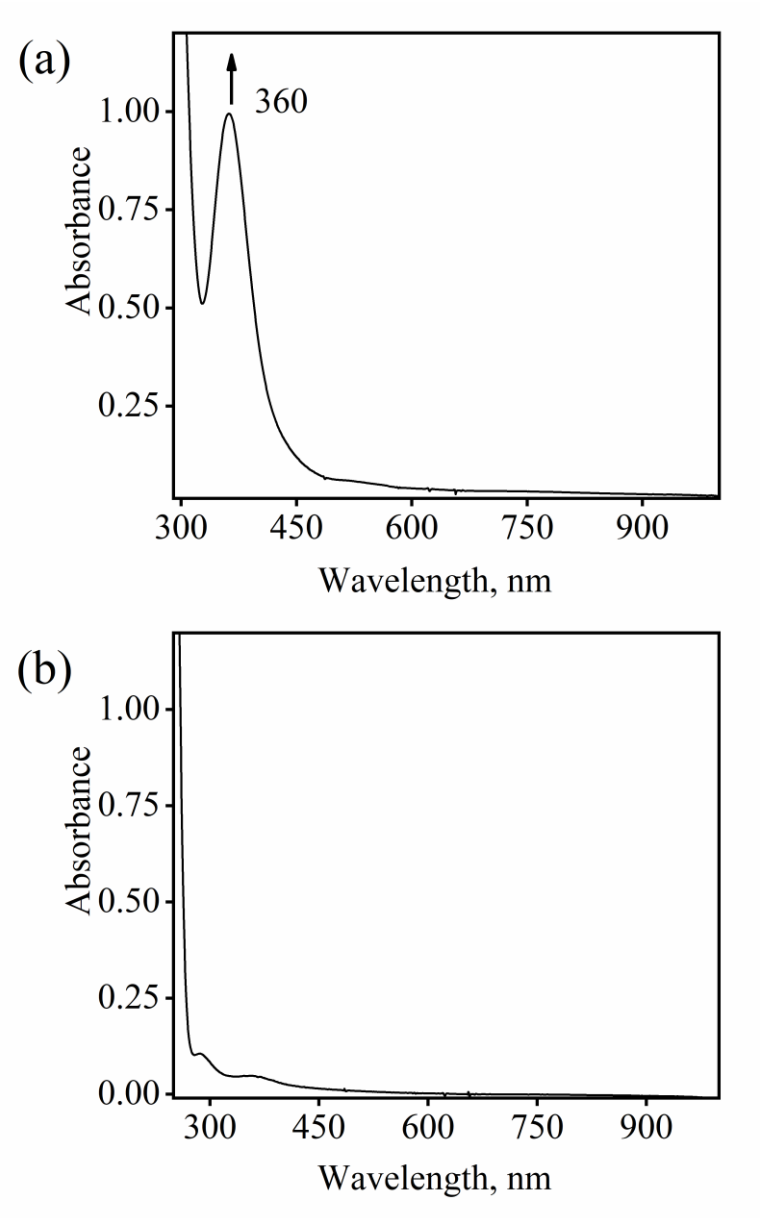

Figure S16. (a) UV-vis spectrum of the reaction mixture of **2** (0.1mM) + H^+ (0.1 mM) + sodium iodide (0.15 mM) in CH_3CN at 298 K. (b) UV-vis spectrum of the reaction mixture of **2** (0.1 mM) + H^+ (0.2 mM) + sodium iodide (0.15 mM) in CH_3CN at 298 K.

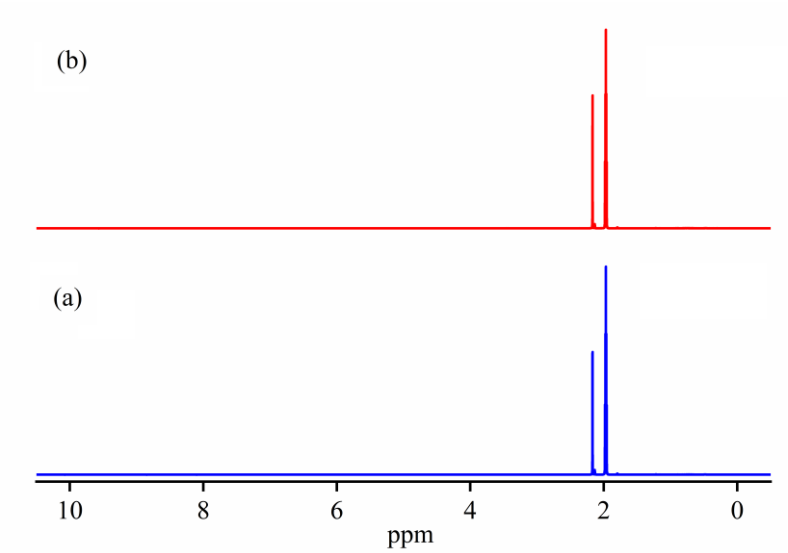

Figure S17. ^{1}H-NMR (400 MHz) spectra of (a) **2** (10 mM) and (b) **2** (10 mM) + D^{+} (20 mM) in CD_3CN at RT.

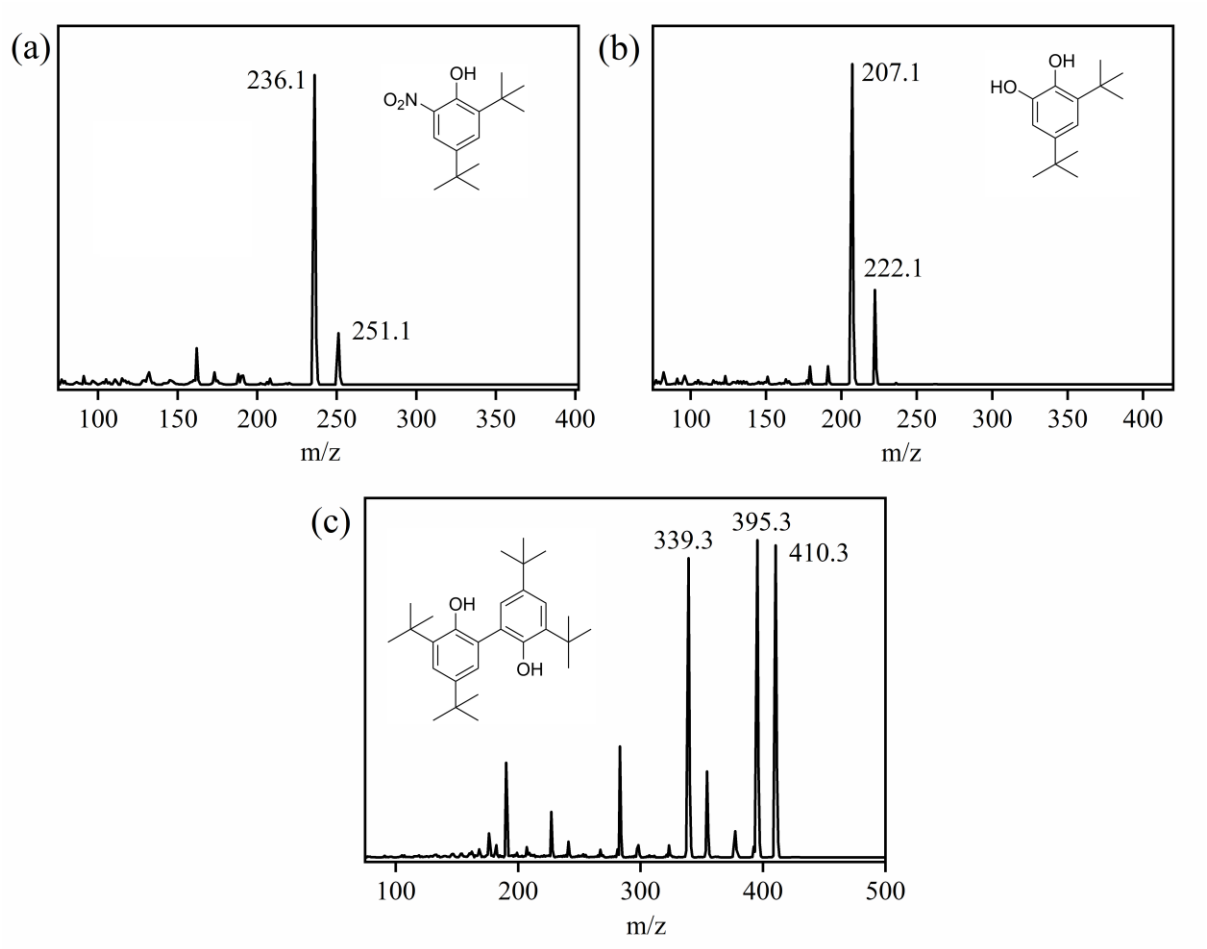

Figure S18. GC-MS characterization of the reaction mixture of **2** (1mM) + one equiv. of H^+ (1mM) + 2,4-DTBP (2.5mM). (a) nitro-2,4-DTBP (nitro-2,4-DTBP): The peaks at *m/z* 251.1 and 236.1 are assigned to be nitro-2,4-DTBP and loss of CH_3 from nitro-2,4-DTBP. (b) 3,5-Di-*tert*-butylcatechol (3,5-DTBC); The peak at *m/z* value 222.1, 207.1 are assigned to 3,5-DTBC and CH_3 loss from 3,5-DTBC respectively. (c) 2,4-DTBP-dimer (2,4-DTBP-D); The peaks at *m/z* 410.3, 395.3, and 339.3 are assigned to be 2,4-DTBP-D, loss of CH_3 from 2,4-DTBP-D, loss of C_4H_8 and CH_3 from 2,4-DTBP-D. The peaks were compared with the NIST standard library.

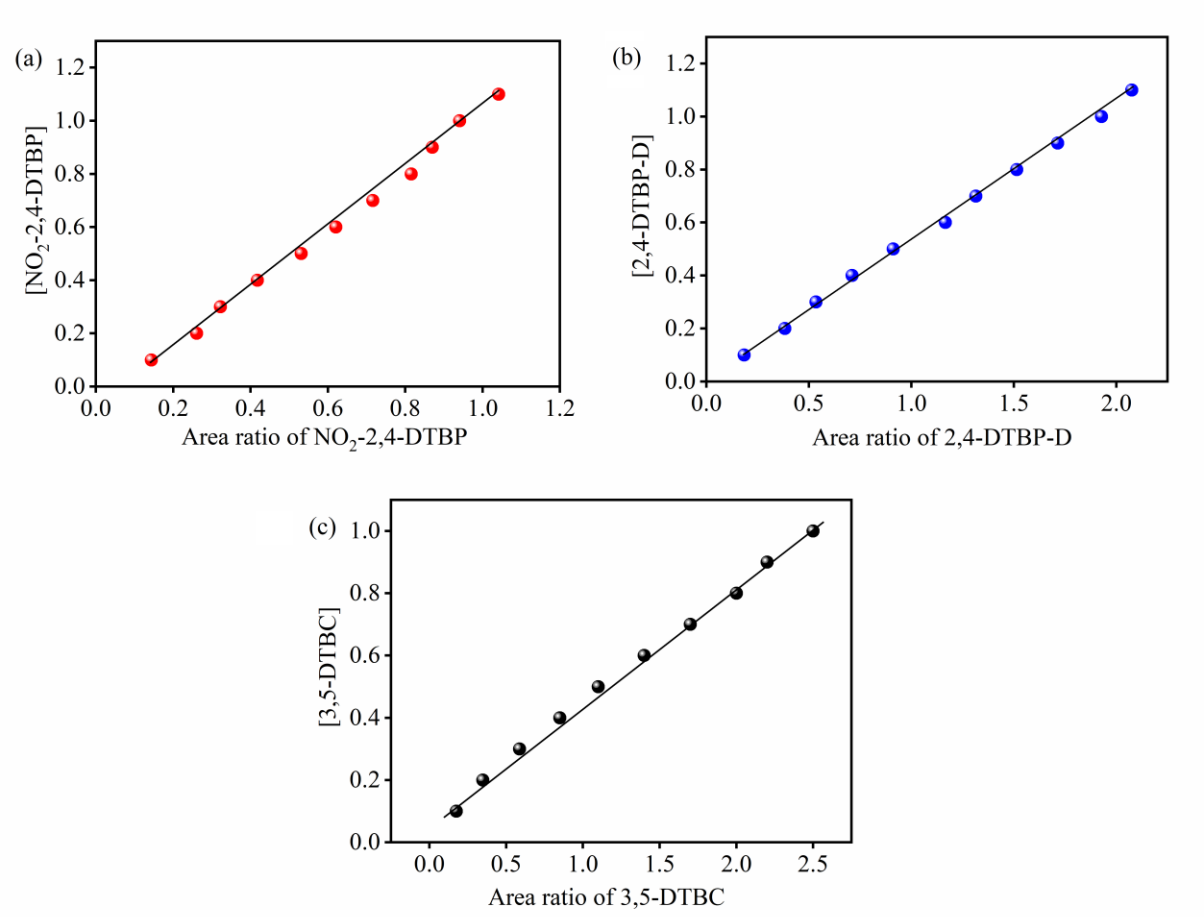

Figure S19. HPLC calibration plot for (a) nitro-2,4- DTBP, (b) 2,4-DTBP-D, and (c) 3,5-DTBC.

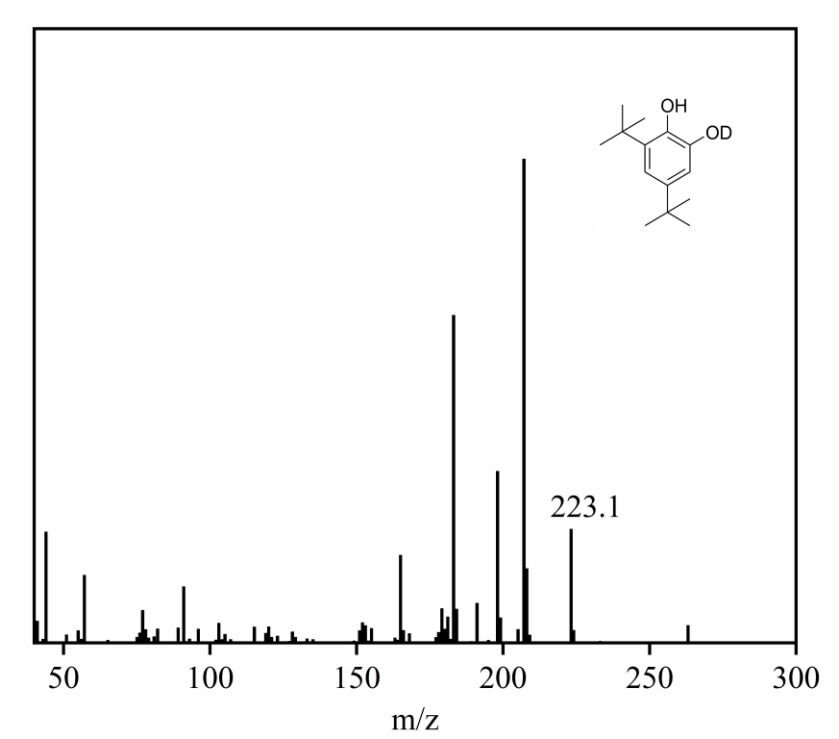

Figure S20. GCMS characterization of 3,5-DTBC(D) from the reaction mixture of **2** (1mM) + one equiv. of D^+ (1mM) + 2,4-DTBP (2.5mM).

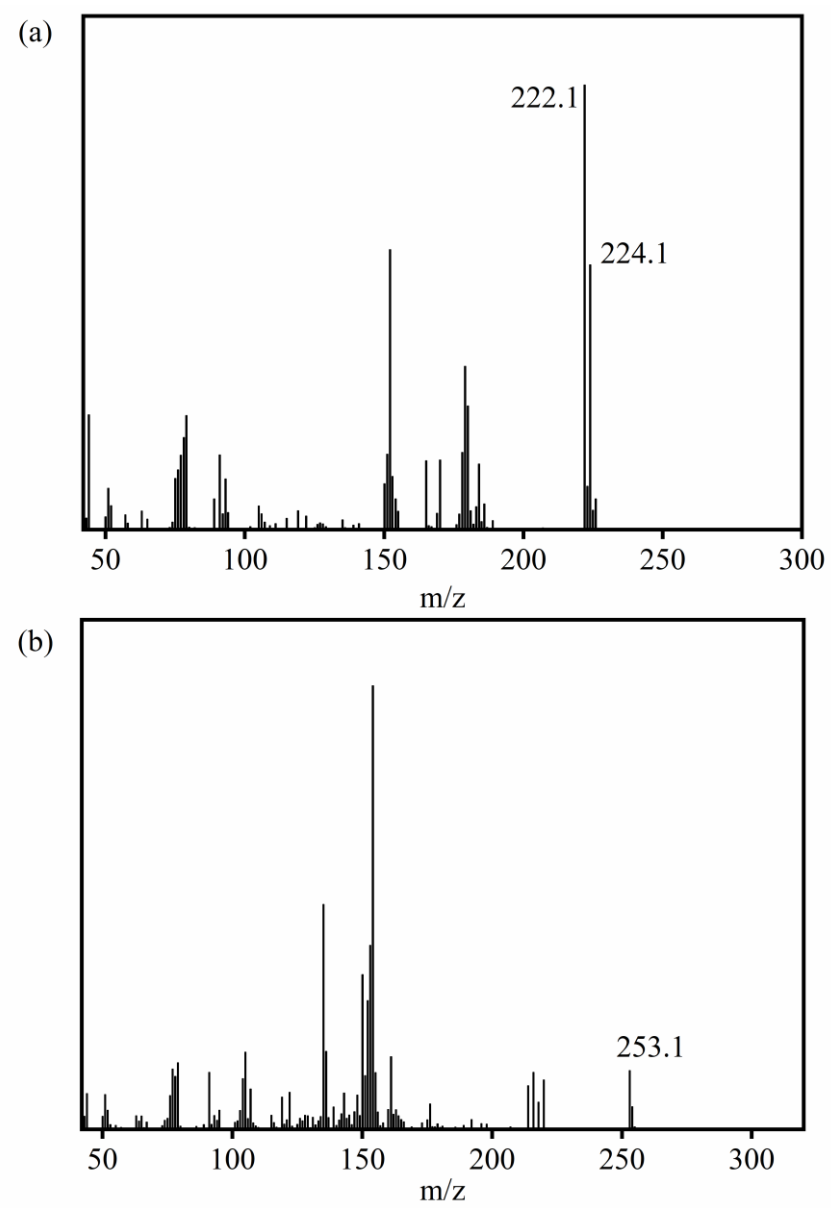

Figure S21. GCMS characterization of (a) 3,5-Di-tert-butylcatechol [3,5-DTBC(^{18}OH)]; The peak at m/z value 224.1, 222.1 are assigned to 3,5-DTBC (^{18}OH) and 3,5-DTBC(^{16}OH) respectively. (b) The peak at 253.1 is assigned to be nitro-2,4-DTBP(^{16}ON^{18}O), in the reaction mixture of **2**-^{16}ON^{18}O^{-} with one equiv. of H^{+}.

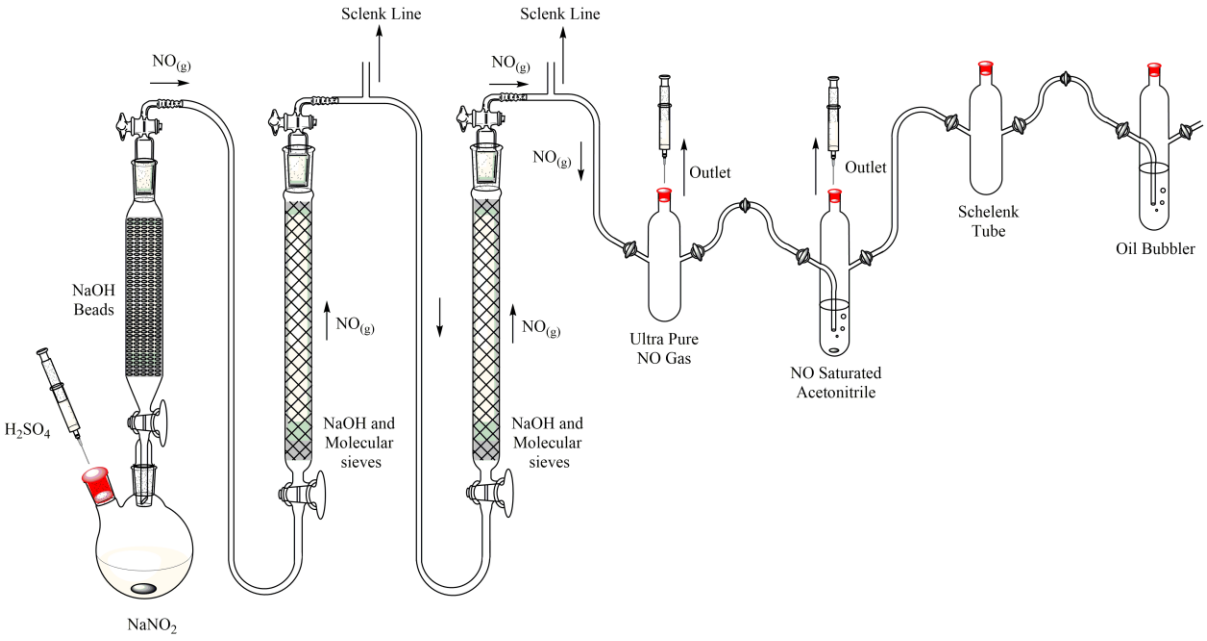

Figure S22. Schematic diagram showing the generation and purification setup for NO.